BIOCHEMISTRY
including biophysical chemistry & molecular biology
Article

Biochemistry **2011,** *50,* 523–532 523
DOI: 10.1021/bi101328r

Nature of the Reaction Intermediates in the Flavin Adenine Dinucleotide-Dependent Epoxidation Mechanism of Styrene Monooxygenase[†]

Auric Kantz and George T. Gassner*

Department of Chemistry and Biochemistry, San Francisco State University, San Francisco, California 94132, United States

Received August 17, 2010; Revised Manuscript Received December 15, 2010

ABSTRACT: Styrene monooxygenase (SMO) is a two-component flavoenzyme composed of an NADH-specific flavin reductase (SMOB) and FAD-specific styrene epoxidase (NSMOA). NSMOA binds tightly to reduced FAD and catalyzes the stereospecific addition of one atom of molecular oxygen to the vinyl side chain of styrene in the enantioselective synthesis of *S*-styrene oxide. In this mechanism, molecular oxygen first reacts with NSMOA(FAD_{red}) to yield an FAD C(4a)-peroxide intermediate. This species is nonfluorescent and has an absorbance maximum of 382 nm. Styrene then reacts with the peroxide intermediate with a second-order rate constant of $(2.6 \pm 0.1) \times 10^6\ M^{-1}\ s^{-1}$ to yield a fluorescent intermediate with an absorbance maximum of 368 nm. We compute an activation free energy of 8.7 kcal/mol for the oxygenation step, in good agreement with that expected for a peroxide-catalyzed epoxidation, and acid-quenched samples recovered at defined time points in the single-turnover reaction indicate that styrene oxide synthesis is coincident with the formation phase of the fluorescent intermediate. These findings support FAD C(4a)-peroxide being the oxygen atom donor and the identity of the fluorescent intermediate as an FAD C(4a)-hydroxide product of the styrene epoxidation. Overall, four pH-dependent rate constants corresponding to peroxyflavin formation (pK_a = 7.2), styrene epoxidation (pK_a = 7.7), styrene oxide dissociation (pK_a = 8.3), and hydroxyflavin dehydration (pK_a = 7.6) are needed to fit the single-turnover kinetics.

Pseudomonas bacteria are equipped with an efficient set of catabolic and detoxification enzymes that allow them to thrive in contaminated environments using a diverse array of aromatic hydrocarbons as sole sources of carbon and energy (*1*). Recently, a common pathway for the catabolism of styrene was identified (*2*). At the entry point of the catabolic pathway, styrene is oxidized through the sequential activities of three enzymes: styrene monooxygenase, which catalyzes the epoxidation of the vinyl side chain of styrene; styrene oxide isomerase, which transforms styrene oxide to phenylacetaldehyde; and phenylacetaldehyde dehydrogenase, which catalyzes the oxidation of phenylacetaldehyde to phenylacetic acid (*2*). Phenylacetic acid is then transformed by enzymes shared in common with the phenylalanine catabolic pathway to yield intermediates of the tricarboxylic acid cycle (*3*, *4*). This pathway is a point of interest for researchers spanning disciplines of microbiology, biotechnology, and mechanistic enzymology (*5*−*16*).

The enzymatic synthesis of *S*-styrene oxide by styrene monooxygenase in the first committed step of this pathway is of particular interest in that it provides insight into the mechanism of a flavin-catalyzed epoxidation reaction, which occurs in an unassisted fashion by metal cofactors and with exceptional enantioselectivity (*2*, *17*). Similar flavin adenine dinucleotide-dependent epoxidation reactions are catalyzed by squalene and zeaxanthin epoxidases in the biosynthesis of cholesterol and plant pigments, but styrene monooxygenase has proven to be the best candidate for mechanistic studies because of technical challenges associated with working with these related systems (*18*, *19*). Styrene monooxygenase (SMO)[1] is a two-component flavoenzyme composed of an NADH-specific reductase, SMOB, and FAD-specific epoxidase, NSMOA (*9*, *14*). SMO is most closely related to the two-component flavin-diffusible systems (*20*), and the epoxidase component is structurally very similar to that of 4-hydroxybenzoate 3-monooxygenase and related flavin monooxygenases (*12*, *16*).

In all studies of flavoprotein monooxygenases in which reaction intermediates have been kinetically resolved, it has been demonstrated that either a flavin C(4a)-peroxide or hydroperoxide is engaged as either a nucleophile (*21*, *22*) or an electrophile (*23*, *24*) in its reaction with substrate. Transfer of an oxygen atom from the flavin peroxide to the substrate results in the production of a C(4a)-hydroxyflavin intermediate, which is dehydrated to yield oxidized flavin in a reaction that is dependent on both pH and ionic conditions (*25*, *26*).

It was previously suggested that a flavin oxaziridine could represent an alternative to the flavin peroxide as a donor of an oxygen atom in flavin-catalyzed monooxygenation reactions (*27*). Computational studies indicate oxaziridine-catalyzed epoxidations proceed through a more asynchronous transition state with

[†]This work was supported by National Institutes of Health Grant GM081140 (G.T.G.).

*To whom correspondence should be addressed: Department of Chemistry and Biochemistry, San Francisco State University, San Francisco, CA 94132. Telephone: (415) 637-1387. Fax: (415) 338-2384. E-mail: gassner@sfsu.edu.

[1]Abbreviations: SMO, styrene monooxygenase; NSMOA, N-terminally histidine-tagged styrene monooxygenase epoxidase component; FAD, flavin adenine dinucleotide; NADH, nicotinamide adenine dinucleotide; NSMOA(FAD_{red}), NSMOA with reduced FAD bound; NSMOA(FAD_{ox}), NSMOA with oxidized FAD bound; NSMOA(FAD_{OOH}), NSMOA with bound FAD C(4a)-hydroperoxide; NSMOA(FAD_{OH}), NSMOA with bound FAD C(4a)-hydroxide; SMOB, styrene monooxygenase reductase component.

© 2010 American Chemical Society
Published on Web 12/17/2010

radical character greater than that computed for peracid-catalyzed alkene epoxidation reactions (*28*). Oxaziridines generally catalyze the epoxidation of substituted alkenes with enantioselectivity greater than what is observed for corresponding reactions of organic peroxides or peracids (*29*), and the possibility that an FAD-oxaziridine could be the intermediate responsible for oxygen atom transfer in the reaction mechanisms of flavoenzyme epoxidases could not be ruled out in our earlier studies of NSMOA (*14*).

Unique flavin products are predicted to result from the flavin oxaziridine- and flavin peroxide-catalyzed reactions. Transfer of an oxygen atom from flavin C(4a)-peroxide results in C(4a)-hydroxyflavin, which then eliminates water to yield oxidized FAD. Transfer of an oxygen atom from flavin oxaziridine results in the production of oxidized flavin without a C(4a)-hydroxyflavin intermediate. Here we use rapid acid quench in conjunction with stopped-flow absorbance and fluorescence studies to resolve the kinetic phase in which styrene oxide is synthesized and the nature of the intermediate responsible for the oxygen atom transfer step of the styrene epoxidation reaction. Activation parameters and pK_a values defining the energetics of the transition states and pH dependence of the kinetic steps in this reaction are presented.

MATERIALS AND METHODS

Expression and Recovery of Recombinant Protein. The N-terminally histdine-tagged version of styrene monooxygenase used in this paper was expressed from the pET-28NSMOA vector in *Escherichia coli* BL21(DE3) cells and purified by nickel affinity chromatography. Purified protein was assayed for specific activity, flavin binding, and redox potential as described previously (*14*).

Single-Turnover Absorbance and Fluorescence Studies. Stopped-flow absorbance and fluorescence studies were completed with previously described single-mixing and double-mixing stopped-flow instruments (*14*, *16*). Single-wavelength absorbance and fluorescence measurements were recorded with a photomultiplier interfaced with a Pico 216 ADC. Diode array spectra were recorded with an HR2000+ Ocean Optics diode array spectrophotometer interfaced with the stopped-flow instrument.

FAD fluorescence was excited in the double-mixing stopped-flow instrument along the 0.35 mm path length of the flow cell by using a xenon-arc lamp filtered through an Edmund Optics U340 filter. In the single-mixing Applied Photophysics stopped-flow instrument, FAD fluorescence was excited via projection of 450 nm light with a 5 nm spectral resolution across the 1 mm path length of the flow cell. In both instruments, fluorescence emission was monitored at a right angle to the excitation light across the 1 cm path length, and stray light was limited with an Edmund Scientific VG6 band-pass filter placed directly in front of the emission photomultiplier tube. Exponential fits through kinetic data recorded in experiments using either stopped-flow fluorescence method return the same set of best fitting rate constants.

In experiments requiring anaerobiosis, we made solutions anaerobic in a glass tonometer equipped with a titration port and a 1 cm path length quartz cuvette by repeatedly evacuating and backfilling the tonometer with purified nitrogen gas on a Schlenk line. Solutions of the reduced NSMOA(FAD_{red}) complex were generated by incremental addition of dithionite from a gastight Hamilton syringe attached to a tonometer.

Styrene, benzene, and flavin solutions were prepared as previously described (*14*). Solutions containing defined concentrations of dissolved oxygen were prepared by mixing appropriate volumes of air-saturated and anaerobic buffers. Experimental data were fit and plotted using Kaliedagraph version 4.02 and GraphPad Prism version 4.0b.

pH Dependence Studies. NSMOA was prepared in 5 mM MOPSO (pH 7) containing 5% glycerol and reacted in 0.1 M MOPSO (pH 6.5), 0.1 M MOPSO (pH 7), 0.1 M HEPES (pH 7.5), 0.1 M HEPES (pH 8), 0.1 M POPSO (pH 8.5), or 0.1 M CHES (pH 9). Buffers included sodium chloride, which gave a final ionic strength of 0.1 M. The actual pH after 1:1 mixing was verified by measurement with a pH probe.

Rapid Acid Quench Studies. The double-mixing stopped-flow instrument was reconfigured for use as a rapid quench instrument via modification of the internal flow path and addition of a sample-aging loop, check valves, an electronically actuated flow-path-switching valve, and a sample-recovery syringe. In the first push, reduced enzyme is mixed with oxygen and styrene as it passes through a fluorescence flow cell and into a delay loop. As buffer is displaced from the aging loop by incoming reactants, it enters and fills the stop syringe. Once filled, the stop syringe impacts the stop block and closes a switch, which initiates the collection of fluorescence data and actuates the flow-path-switching valve to connect the aging loop and sample-recovery syringe. After a user-defined delay time, a second push directs the reacting sample in the aging loop to a second mixer where it is quenched with 2 M HCl. In addition to stopping the progression of the single-turnover reaction, the acid instantly hydrolyzes the styrene oxide to yield α,β-dihydroxyethylbenzene. As the quenched sample exits from the mixer, it passes through the flow-path-switching valve and fills a removable 2.5 mL Hamilton gastight sample-recovery syringe.

Product Derivatization and Detection. Approximately 600 μL of acid-quenched reaction product was immediately injected through a septum into a gastight 10 mL reaction vial containing 450 mg of magnesium sulfate and 10 mg of methylboronic acid to form the methylboronic ester of α,β-dihydroxyethylbenzene. Two minutes after the reaction vial had been vortexed, a 1 mL sample of headspace gas was drawn from the esterification reaction vial and immediately injected into a Varian Saturn 2000 GC−MS/MS system equipped with a 30 m Varian VF-5 ms capillary column. The injector temperature was set to 80 °C, and separation was achieved with a temperature program that began with a 5 min isocratic step followed by a linear temperature gradient from 80 to 250 °C at a heating rate of 4 °C/min. Under these separation conditions, styrene detected at 4.8 min and the methylboronic ester of α,β-dihydroxyethylbenzene detected at 11.7 min were quantified on the basis of their respective total ion intensities monitored at m/z values of 105 and 161, respectively.

RESULTS

Temperature and pH Dependence of the Single-Turnover Reaction of NSMOA(FAD_{red}) with Oxygen and Styrene. The kinetics of the reaction of reduced NSMOA with oxygen and styrene were monitored by single-mixing absorbance and fluorescence stopped-flow spectroscopy over a range of pH values. Representative kinetic traces from experiments conducted at pH 6.4 and 8.8 are shown in panels A and B of Figure 1, respectively. A total of four exponentials were required to globally fit the fluorescence and absorbance data at each pH, and each of the four resulting rate constants was found to be dependent on pH. Lines passing through the data in panels A and B of Figure 1 represent the best sequential four-exponential fits through these data as a function of pH (*30*).

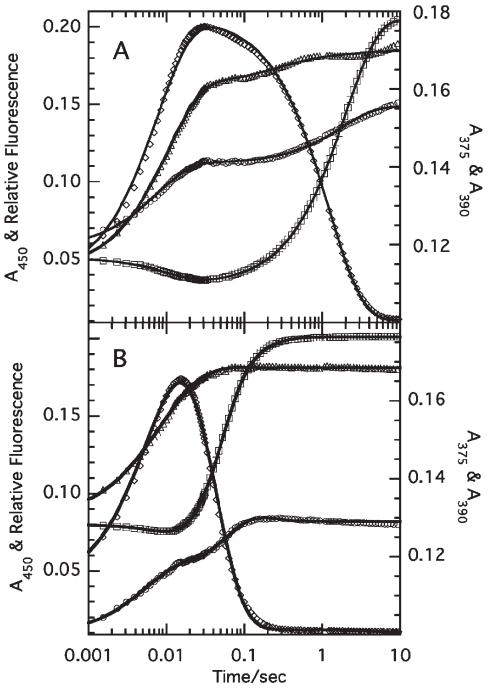

FIGURE 1: Reaction of NSMOA with styrene and oxygen monitored by absorbance and fluorescence. Data for the reaction of 25 μM NSMOA(FAD_{red}) with 134 μM oxygen and 125 μM styrene at 25 °C monitored by absorbance at (△) 375, (○) 390, and (□) 450 nm and by fluorescence emission at 520 nm (◇). Data representative of the reaction kinetics at pH 6.4 and 8.8 are shown in panels A and B, respectively. Solid lines represent the best exponential fits through the data. Relative fluorescence intensities are scaled to allow comparison with absorbance data.

pK_a values corresponding to each of these rate constants were computed by fitting observed rate constants as functions of pH according to eq 1.

$$k_{obs} = \frac{k_{high}}{1 + 10^{pK_a - pH}} + \frac{k_{low}}{1 + 10^{pH - pK_a}} \quad (1)$$

Best fits passing through the data over the temperature range of 15−25 °C are given in Figure 2. pK_a values and limiting values of the observed rate constants resulting from these fits are listed in Table 1. Activation parameters associated with the computed values of observed rate constants at limiting values of low and high pH (Table 2) were estimated from the best linear fits through Eyring plots (Figure 3A−D). Thermodynamic parameters associated with the kinetically resolved macroscopic pK_a values in the single-turnover reaction (Table 3) were estimated from the best linear fits through the van't Hoff plots (Figure 3E−H) (*31*).

pH Dependence of the Spectra of Kinetic Intermediates in the Epoxidation Reaction. Time-resolved absorbance spectra representative of the peroxide and hydroxide intermediates were recorded each with an 8 ms integration time by diode array spectroscopy 100 ms after mixing. After subtraction of the spectral contribution of free oxidized FAD present in each sample, it was possible to obtain spectra representative of the intermediates occurring in the reaction of oxygen and styrene with the reduced enzyme (Figure 4). These spectra have absorbance maxima of 382 and 368 nm, respectively, that are independent of pH in the range of 6−9.

Identification of the Kinetic Phase Associated with Styrene Oxide Synthesis. A time course for the evolution of kinetic intermediates in the reaction of NSMOA with oxygen and

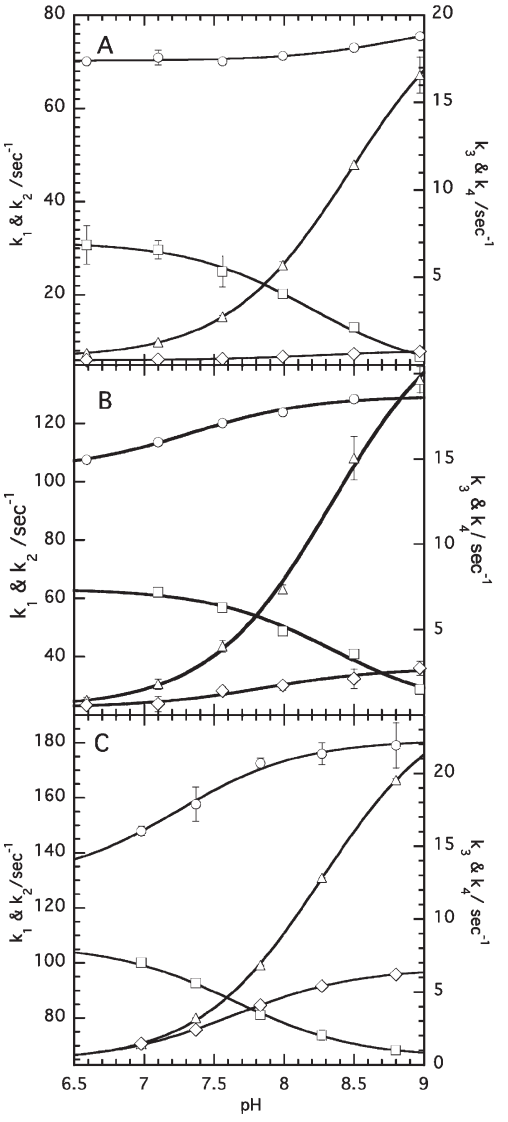

FIGURE 2: pH and temperature dependence of the observed rate constants from the reaction of NSMOA with oxygen and styrene. Rate constants (○) k_1, (□) k_2, (△) k_3, and (◇) k_4 estimated by exponential fitting of time-resolved absorbance and fluorescence data. Solid curves passing through the data represent the best fits of the observed rate constants as a function of pH at 15, 20, and 25 °C (A−C, respectively).

Table 1: Limiting pH-Dependent Rate Constants and pK_a Values at 25 °C

rate constant	low-pH limit (s^{-1})	high-pH limit (s^{-1})	associated pK_a
k_1	129 ± 4.9	182 ± 3.7	7.2 ± 0.2
k_2	107 ± 0.8	65.6 ± 0.8	7.7 ± 0.1
k_3	0.2 ± 0.08	25.2 ± 0.03	8.3 ± 0.1
k_4	0.2 ± 0.1	6.6 ± 0.1	7.6 ± 0.1

styrene is given in Figure 5. Concentrations of species computed by using best fitting rate constants from kinetic fitting at pH 7 and 25 °C and the integrated rate expression for a sequential four-exponential reaction (*30*) are shown as solid lines. The solid line marked by a filled circle shows the formation and decay kinetics of the fluorescent intermediate. Dashed lines contrast the computed time courses expected if styrene oxide synthesis is coupled to the formation (marked by a solid triangle) or decay (marked by a hollow triangle) of the fluorescent intermediate. Empty circles with error bars show the relative yield of styrene oxide 0.1 and

Table 2: Activation Parameters in the Styrene Epoxidation Mechanism of NSMOA at 25 °C

rate constant	$\Delta G^{\ddagger}_{(\text{low pH})}$ (kcal/mol)[a]	$\Delta G^{\ddagger}_{(\text{high pH})}$ (kcal/mol)[a]	$\Delta H^{\ddagger}_{(\text{low pH})}$ (kcal/mol)	$\Delta H^{\ddagger}_{(\text{high pH})}$ (kcal/mol)	$T\Delta S^{\ddagger}_{(\text{low pH})}$ (kcal/mol)	$T\Delta S^{\ddagger}_{(\text{high pH})}$ (kcal/mol)
k_1	14.3 ± 0.5	14.3 ± 0.5	9.8 ± 1.4	13.3 ± 1.2	−4.7 ± 0.8	−1.0 ± 0.1
k_2	14.4 ± 0.1	14.4 ± 0.1	20.3 ± 1.6	51.1 ± 7.5	5.7 ± 0.5	36.1 ± 5.5
k_3	18.2 ± 9.1	15.3 ± 0.1	−9.2 ± 7.0	1.9 ± 0.8	−27.5 ± 14.6	−13.6 ± 23.1
k_4	8.2 ± 7.3	16.1 ± 2.0	−1.9 ± 10.4	34.3 ± 2.5	−20.1 ± 35.3	18.1 ± 1.4

[a]Calculated using the equation $\Delta G^{\ddagger} = -RT \ln[h/(k_B T)k_{obs}]$ and the rate constants listed in Table 1.

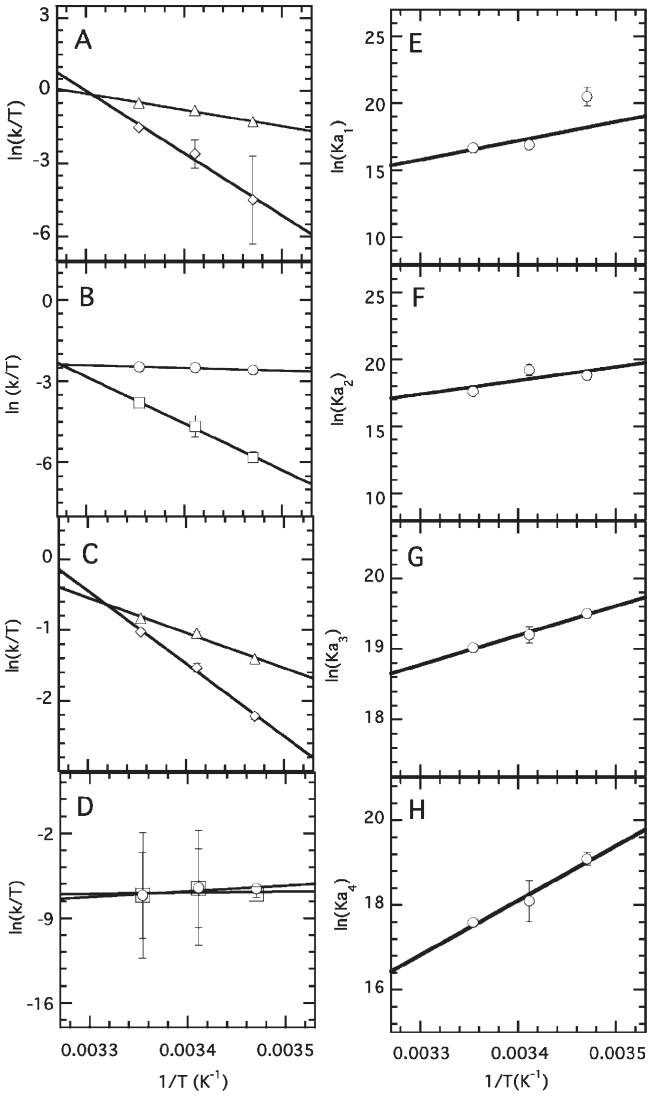

FIGURE 3: Energetic analysis of observed rate constants and kinetically resolved K_a values in the reaction mechanism of NSMOA. Eyring plots of limiting values of rate constants (△) k_1 and (◇) k_2 at low pH (A) and high pH (C). Limiting values of rate constants (○) k_3 and (□) k_4 at low pH (B) and high pH (D). van't Hoff plots of the macroscopic K_a values associated with each observed rate constant are shown in panels E−H.

1 s after mixing detected by GC−MS as the methylboronic ester of α,β-dihydroxyethylbenzene.

Binding of Benzene to the FAD C(4a)-Peroxide Intermediate of NSMOA. When NSMOA(FAD_{red}) is rapidly mixed in the stopped-flow instrument with oxygen, a rapid increase in absorbance at 375 nm corresponding to the formation of flavin peroxide is observed. In the 100 ms to 10 s time range, the 450 nm absorbance increases as hydrogen peroxide is eliminated slowly to regenerate the spectrum of oxidized flavin.

Table 3: Ionization Energy Parameters of Kinetically Resolved K_a Values at 25 °C

kinetically resolved pK_a	ΔG (kcal/mol)[a]	ΔH (kcal/mol)	$T\Delta S$ (kcal/mol)
pK_{a1}	9.8 ± 0.3	28.2 ± 8.1	18.4 ± 8.1
pK_{a2}	10.5 ± 0.1	20.2 ± 19.7	9.6 ± 20.1
pK_{a3}	11.3 ± 0.1	8.2 ± 1.0	−3.0 ± 1.1
pK_{a4}	10.4 ± 0.1	25.6 ± 4.5	15.2 ± 4.6

[a]Calculated using the equation $\Delta G^{o\prime} = 2.303RT \times pK_a$ and rate constants listed in Table 1.

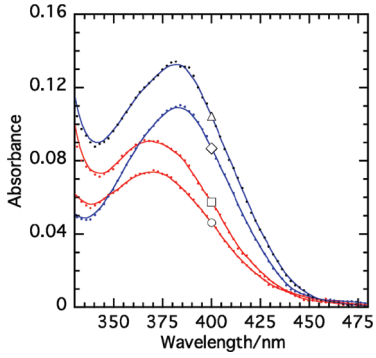

FIGURE 4: Time-resolved spectra representative of flavin peroxide and hydroxide intermediates detected in the epoxidation reaction of NSMOA. The top pair of spectra (blue) are representative of the peroxide intermediate recorded 100 ms after reduced FAD-bound NSMOA had been mixed with oxygen at (◇) pH 6.4 and (△) pH 8.8. The bottom pair of spectra (red) are representative of the hydroxide intermediate recorded 100 ms after reduced FAD-bound NSMOA had been mixed with oxygen and styrene at (□) pH 6.4 and (○) pH 8.8. Lines are smooth fits through the data provided for the sake of clarity.

The substrate analogue benzene has no significant effect on the kinetics of FAD C(4a)-peroxide formation but has a significant stabilizing effect that greatly increases the half-life of the peroxide intermediate (Figure 6A). Because the observed rate constant of formation of NSMOA(FAD_{OOH}) is much larger than the decay rate constant, the total enzyme and benzene concentrations involved in the decay reaction are well approximated by eqs 2 and 3.

$$[\text{NSMOA}]_T = [\text{NSMOA}(\text{FAD}_{OOH})]_{Free} + [\text{NSMOA}(\text{FAD}_{OOH})\cdot\text{benzene}] \quad (2)$$

$$[\text{benzene}]_T = [\text{benzene}]_{Free} + [\text{NSMOA}(\text{FAD}_{OOH})\cdot\text{benzene}] \quad (3)$$

The absorbance data plotted in Figure 6B correspond to the values recorded in Figure 6A 100 s after mixing. Equations 2 and 3 were combined to allow derivation of eq 4, which makes the approximation that benzene (B) binds with the enzyme peroxide intermediate of NSMOA (A) in a rapid equilibrium (K_{d8}) with respect to the decomposition rate constant of the peroxide

intermediate, and that benzene-bound NSMOA(FAD_{OOH}) represents a dead-end complex.

$$A_{450} = A_{450}^{FAD_{ox}} - \left\{ [K_{d8} + [A]_T + [B]_T - \sqrt{(K_{d8}+[A]_T+[B]_T)^2 - 4[A]_T[B]_T} \right] / 2 \} \varepsilon l \quad (4)$$

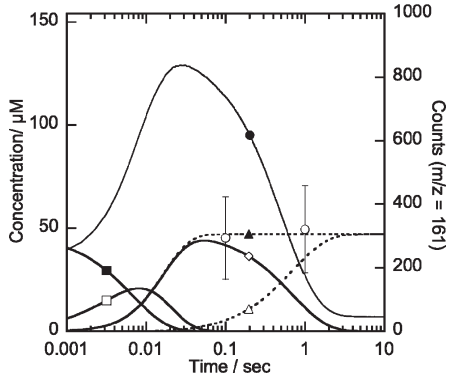

FIGURE 5: Identification of the reaction phase coupled to the synthesis of styrene oxide. Computed concentration profiles showing the transformation of (■) the reduced enzyme to yield first (□) FAD peroxide and then (◇) the fluorescent intermediate observed after the reaction of NSMOA with oxygen and styrene. Dashed lines indicate the time dependence of styrene oxide production if the fluorescent intermediate is (▲) a product of or (△) responsible for the epoxidation reaction. A plot of the experimentally observed reaction fluorescence (●) is included for direct comparison to the concentration profile. Rapid quench time points (○) recovered 0.1 and 1 s after mixing and assayed by GC−MS.

The complete set of species involved in this transformation is given in Figure 7, and the subset of direct significance to the NSMOA(FAD_{OOH}) decomposition reaction is enclosed within the dashed rectangle. K_d values 1−4 (*16*) represent rapid equilibria with respect to the NSMOA(FAD_{OOH}) decomposition rate constant. Thus, immediately following decomposition of the peroxide intermediate, the enzyme can be described by the subset of states related through K_{d1}−K_{d4} (Figure 7). The extinction coefficient (ε) in eq 4 does not discriminate between the free and bound forms of oxidized FAD presented in this model. The best fitting values of K_{d8} and ε are 62.7 ± 4.7 μM and 9.6 ± 0.1 mM^{-1} cm^{-1}, respectively.

Chloride Effect in the Epoxidation Mechanism of NSMOA. Observed rate constants (k_2 and k_3) (Table 1) corresponding to the kinetics of formation and decay of the fluorescent intermediate observed in the epoxidation reaction are dependent on ionic conditions (Figure 8A). As the sodium chloride concentration is increased from 0 to 1 M, the formation rate constant decreases linearly and the rate constant for the decay of the fluorescent intermediate decreases hyperbolically. The best hyperbolic fit through the data indicates the decay rate constant decreases from 2.83 s^{-1} in the absence of added salt to a limiting value of 0.013 s^{-1}. A salt concentration of 162 ± 13 mM results in half of the maximum inhibitory effect.

Determination of the Second-Order Rate Constant for the Reaction of NSMOA(FAD_{OOH}) with Styrene. The kinetics of the reaction of the FAD C(4a)-peroxide intermediate with styrene were examined by double-mixing stopped-flow fluorescence spectroscopy. In these studies, NSMOA(FAD_{red})

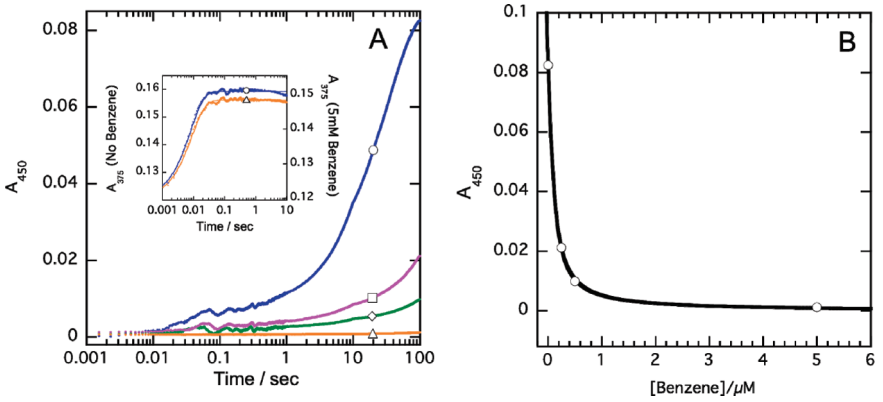

FIGURE 6: Stabilization of the flavin peroxide intermediate by benzene. Panel A shows the absorbance changes at 450 nm (0.1 cm path length) corresponding to the reaction of 86 μM NSMOA(FAD_{red}) at 25 °C with 0.1 M air-saturated MOPSO (pH 7) containing (○) 0, (□) 0.25, (◇) 0.5, and (△) 5 mM benzene. The inset shows the kinetics of the same reaction monitored at 375 nm in the presence (△) or absence (○) of 5 mM benzene. In panel B, the absorbance recorded at 450 nm, 100 s after mixing, is fit as a function of benzene concentration as described in the text.

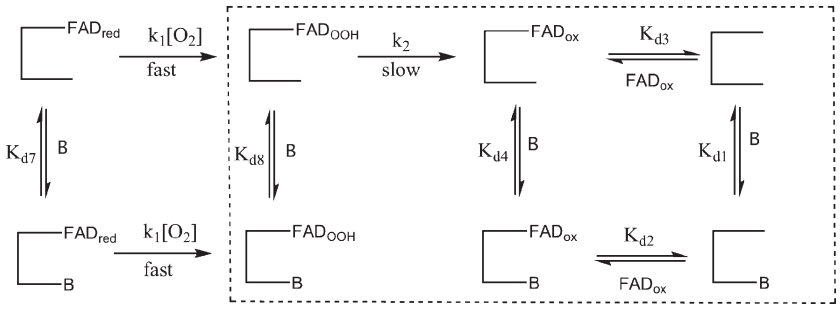

FIGURE 7: Ligand binding equilibria in the NSMOA(FAD_{OOH}) decomposition reaction. At submillimolar benzene concentrations, the enzyme partitions primarily into benzene-bound forms of NSMOA(FAD_{OOH}) and NSMOA(FAD_{ox}). The benzene binding reactions presented occur rapidly on the time scale of the NSMOA(FAD_{OOH}) decomposition reaction. K_{d1}, K_{d3}, and K_{d7} are all greater than 1 mM. K_{d2}, K_{d4}, and K_{d8} are each in the range of tens of micromolar.

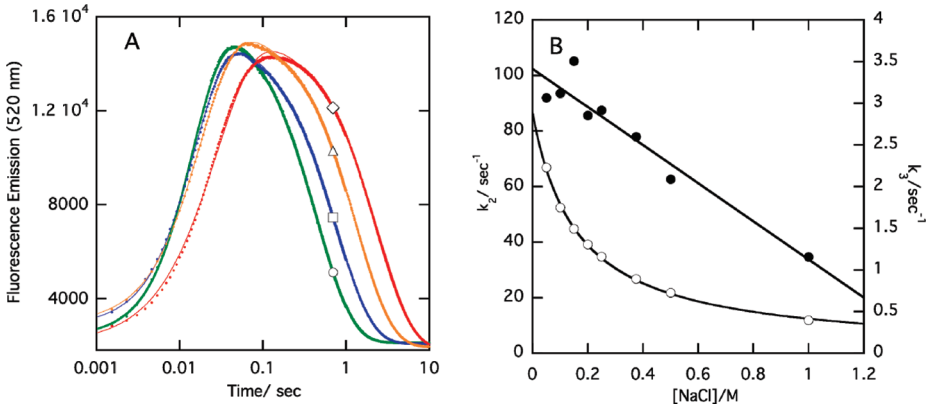

FIGURE 8: Dependence of epoxidation kinetics on solution ionic strength. (A) Fluorescence data recorded after 50 μM NSMOA(FAD_{red}) had been mixed with aerobic 0.1 M MOPSO buffer (pH 7) containing 250 μM styrene and (○) 0, (□) 0.1, (△) 1, and (◇) 2 M NaCl at 25 °C. (B) Rate constants from exponential fitting of the fluorescent intermediate (●) formation and (○) decay plotted as a function of NaCl concentration.

was rapidly mixed with aerobic buffer to generate the peroxide intermediate. After a 100 ms delay time, the peroxide intermediate generated in the first push was rapidly mixed with aerobic buffer containing various amounts of styrene (Figure 9). Two kinetic reaction phases corresponding to the styrene-dependent formation of the NSMOA(FAD_{OH}) intermediate followed by the styrene-independent dehydration of this intermediate to yield oxidized FAD were observed. Reaction conditions were second-order considering the similar concentrations of the styrene and NSMOA(FAD_{OOH}) reacted in this study, and the overall reaction was fit using eq 5, which represents the sum of equations corresponding to a second-order styrene-dependent formation and first-order styrene-independent decay of fluorescence.

$$F_t = \frac{[FAD_{OOH}]_0 - [styrene]_0 e^{([FAD_{OOH}]_0 - [styrene]_0)k_{sty}t}}{1 - e^{([FAD_{OOH}]_0 - [styrene]_0)k_{sty}t}} \varepsilon_1 l + f e^{-k_3 t} + \text{const} \quad (5)$$

The four data sets presented in Figure 9 were fit simultaneously at all styrene concentrations with this equation by using the nonlinear curve fitting program GraphPad Prism version 4.0b. In the fit, the rate constants for the formation and decay of fluorescence, k_{sty} and k_3, respectively, and the fluorescence extinction coefficient of the FAD (ε_1) were globally constrained to return the same best-fitting values for each of the data sets. The path length (l) was 0.5 cm for fluorescence emission. The best fit through the data returned the following values: $k_{sty} = (2.6 \pm 0.1) \times 10^6\ M^{-1}\ s^{-1}$, and $k_3 = 1.7 \pm 0.01\ s^{-1}$.

DISCUSSION

Reaction of NSMOA with Reduced Flavin, Oxygen, and Styrene. The binding affinity of NSMOA for reduced FAD is very high (210 nM) and for the oxidized FAD very weak (1.6 mM) (Scheme 1) (*16*). This thermodynamic linkage of ligand binding and redox equilibria is critical to efficient catalysis by this system in that it allows the enzyme to efficiently scavenge reduced flavin from solution and minimize the nonproductive reaction of dissolved oxygen with free flavin and to release oxidized FAD at the end of the catalytic cycle.

When NSMOA(FAD_{red}) is rapidly mixed with oxygen in the presence of 5 mM benzene, the kinetics of flavin peroxide formation are unaffected as shown in the inset of Figure 6A. Our previous ligand binding studies (*16*) indicate the equilibrium dissociation constant of benzene and NSMOA(FAD_{red}) is quite

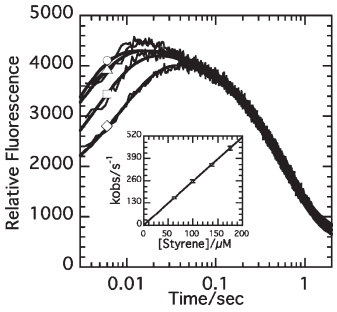

FIGURE 9: Reaction of the FAD C(4a)-peroxide intermediate of NSMOA with styrene. NSMOA(FAD_{red}) (99.6 μM) was first mixed (1:1) with aerobic buffer to generate 49.8 μM FAD-peroxide intermediate. After reaction for 100 ms, the resulting NSMOA(FAD-peroxide) intermediate was mixed (1:1) with various concentrations of styrene in 0.1 M MOPSO buffer (pH 7). Time-dependent changes in fluorescence emission from single-turnover reactions of NSMOA-(FAD-peroxide) with (◇) 63, (□) 100, (△) 138, and (○) 175 μM styrene. Curves passing through the data represent the best global fits through the data set. The inset shows the linear dependence of the observed rate constant of the fluorescence formation phase on styrene concentration.

weak (K_{d7} = 2.3 mM). In the submillimolar benzene concentration range, only a small fraction of available NSMOA(FAD_{red}) active sites are expected to be occupied by benzene. However, at 5 mM benzene, we would expect ~68% occupancy. The fact that we see no inhibition of the peroxide formation kinetics under these conditions suggests that bound benzene does not block access of oxygen to the reduced enzyme or significantly influence the kinetics of the peroxide formation reaction. Given the close structural relationship of benzene and styrene, it is reasonable to conclude that styrene and oxygen similarly react with NSMOA-(FAD_{red}) in a random order.

We find that benzene binds to the NSMOA(FAD_{OOH}) intermediate with a K_d of 62.7 μM (Figure 6B). This represents an increase in affinity of nearly 40-fold over the binding affinity of the reduced enzyme for the substrate analogue, benzene. This increase in active site affinity affords the NSMOA(FAD_{OOH}) state of the enzyme a significantly enhanced ability to bind and react with substrate. We previously estimated the K_i of benzene to be ~173 μM by steady-state kinetic inhibition studies (*14*). This value is quite similar to the value of K_{d8} determined here and suggests that in the steady-state kinetic studies styrene and benzene were probably competing primarily for the NSMOA-(FAD_{OOH}) state of the enzyme.

Scheme 1: Intermediates in the Epoxidation Mechanism of NSMOA

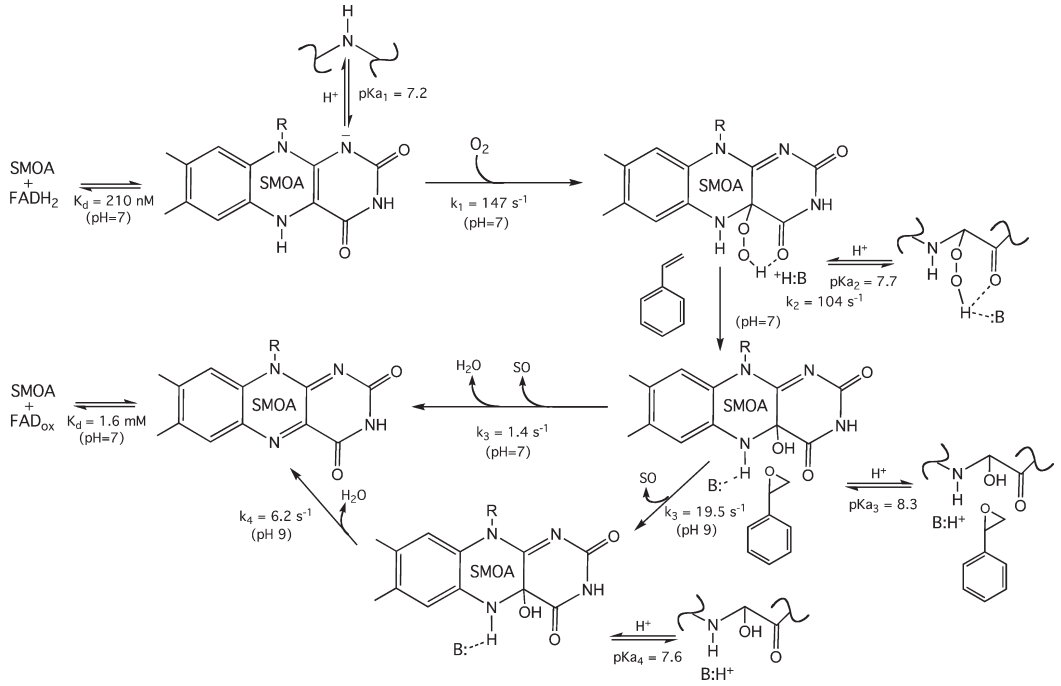

In the double-mixing stopped-flow studies of the reaction of styrene with the peroxide intermediate, we first prepared NSMOA(FAD_{OOH}) by mixing NSMOA(FAD_{red}) with aerobic buffer in the absence of styrene. Once formed, NSMOA(FAD_{OOH}) was rapidly mixed with styrene, and the kinetics of the reaction were monitored. The single-mixing stopped-flow studies involved a different order of substrate addition. The reduced enzyme was premixed with styrene under anaerobic conditions and then rapidly mixed with oxygen. On the basis of the fits presented in Figure 2C, we calculate an observed pseudo-first-order rate constant (k_2 = 104 s^{-1}) for the epoxidation reaction. Dividing this rate constant by the styrene concentration used in this study (125 μM) gives an estimate of the second-order rate constant for the reaction of styrene with the peroxide intermediate equal to 8.3×10^5 M^{-1} s^{-1}, which is a factor of ~3 lower than the value we obtained for k_{sty} in the double-mixing stopped-flow investigation. This is a very slight difference in terms of the free energy of activation but suggests that the peroxide intermediate formed in the absence of bound styrene in the double-mixing stopped-flow experiment may be slightly more reactive than the corresponding intermediate, which forms in the presence of styrene in the single-mixing stopped-flow studies.

Identification of FAD C(4a)-Peroxide as the Oxygen Atom Donor in the Epoxidation Reaction. Flavin C(4a)-peroxides have been identified as the key reaction intermediates responsible for substrate oxygenation by flavin monooxygenases. Transfer of an oxygen atom to the substrate is coupled to the synthesis of the C(4a)-flavin hydroxide intermediate, which eliminates water to regenerate oxidized flavin (*32*). In early theoretical investigations, a flavin oxaziridine was proposed as an alternate candidate oxygen atom donor in the reaction mechanism of flavoprotein monooxygenases (*27*). This intermediate could form through protonation of a flavin C(4a)-peroxide intermediate followed by the elimination of the oxygen atom distal to the flavin as water and cyclization to form an oxaziridine with the proximal oxygen atom bridging the N(5) and C(4a) positions of the flavin. Oxaziridines have demonstrated value as reagents in epoxidation reactions where they have superior enantioselectivity when compared to organic peroxides (*29*). However, flavin oxaziridines have not been prepared synthetically, and on the basis of computational studies, the transition state of an oxaziridine-catalyzed epoxidation is expected to require significantly more activation energy than the corresponding transition state of an organic peroxide-catalyzed epoxidation (*28*). By using the second-order rate constant ($k_{sty} = 2.6 \times 10^6 \pm 0.1$ M^{-1} s^{-1}) and a standard-state reactant concentrations of 1 M at 25 °C, the free energy of activation for the styrene epoxidation reaction is computed to be ~8.7 kcal/mol. This value is in greater agreement with the calculated transition-state free energy of the epoxidation of propylene by performic acid (12.0 kcal/mol) compared with that of the oxaziridine-mediated epoxidation reaction (31.4 kcal/mol) as estimated by computational methods (*28*).

The NSMOA(FAD_{OH}) intermediate is expected to be synthesized only in a flavin peroxide-catalyzed epoxidation of styrene, so its presence can be used to definitively rule out flavin oxaziridine as a reaction intermediate. In considering the defining spectral features reported in the literature for flavin−oxygen intermediates, the flavin C(4a)-peroxide spectrum is generally reported to be red-shifted (380 ± 6 nm) relative to flavin hydroxide (375 ± 10 nm) spectra (*21*, *23*, *24*, *33*−*39*). Intermediates identified as flavin C(4a)-hydroperoxides may be fluorescent (*23*) or nonfluorescent depending on the active site environment, whereas flavin hydroxides are often reported to be highly fluorescent (*39*). In addition, the elimination of water from hydroxyflavin to yield oxidized flavin occurs in a reaction that is quite sensitive to both pH and ionic conditions (*24*−*26*, *40*). Because no model compound information is available regarding the absorbance and fluorescence properties of flavin oxaziridine, or how pH or ionic conditions might affect the reactivity of flavin oxaziridine, we could not use these properties alone to argue for or against the possible role of flavin oxazaridine in the epoxidation mechanism of NSMOA.

We find that the reaction of NSMOA(FAD_{red}) with oxygen and styrene first yields a C(4a)-flavin peroxide, with a peak

absorbance of 382 nm, which is then transformed into a second intermediate with a peak absorbance of 368 nm (Figure 4). In separate studies in which the reaction kinetics were monitored by fluorescence in the absence of styrene and in the presence or absence of benzene as a substrate analogue, it was established that the first intermediate is nonfluorescent and that the second, fluorescent intermediate forms only in the presence of the substrate, styrene. By analyzing acid-quenched reaction mixtures and assaying for styrene oxide, we were able to establish that the synthesis of styrene oxide is coupled to the formation phase of this reaction and that the decay of fluorescence takes place after styrene oxide is synthesized (Figure 5). On the basis of this analysis, we conclude that the fluorescent intermediate we are observing is an FAD C(4a)-hydroxide rather than the FAD oxaziridine and conclude that epoxidation of styrene occurs through a direct transfer of an oxygen atom from the FAD C(4a)-peroxide to styrene.

In the absence of styrene, the peroxide intermediate decomposes to yield hydrogen peroxide and oxidized flavin at a rate of ~0.1 s^{-1} at 25 °C and pH 7. This decomposition rate constant is more than 1 order of magnitude smaller than the rate constant for the release of oxidized flavin in the single-turnover reaction of NSMOA with styrene, suggesting the active site environment plays an important role in stabilizing the FAD C(4a)-peroxide intermediate in the absence of substrate. We have not observed the significant substrate inhibition of the C(4a)-hydroxyflavin dehydration reaction observed in the mechanisms of parahydroxybenzoate hydroxylase (*24*) and 4-hydroxyphenylacetate 3-monooxygenase (*37*). However, we propose that the dissociation of styrene oxide from the hydroxyflavin intermediate state of NSMOA similarly allows exposure of flavin to solvent in a step that promotes subsequent elimination of water to yield oxidized FAD. Dissociation of styrene oxide from the hydrophobic active site of NSMOA is expected to be coupled to a significant ordering of solvent molecules as both the styrene oxide and active site are hydrated. This may be in part responsible for the large negative entropy of activation associated with k_3 in Table 2 . This sequence of events is presented in Scheme 1 together with observed rate constants corresponding to each reaction step.

Dependence of Single-Turnover Reaction Kinetics on Ionic Conditions. Earlier studies of flavoprotein hydroxylases have demonstrated a significant dependence of the kinetics of monooxygenation on azide, iodide, and chloride ions (*24*, *26*, *41*). The C(4a)-hydroxyflavin dehydration reaction is particularly sensitive to interference by anions, and it has been suggested that anions may inhibit this step by blocking the deprotonation of the N(5) position of the flavin (*26*). We also find that the observed rate constant for the hydroxyflavin dehydration reaction decreases hyperbolically as a function of increasing chloride concentration, which provides support for the existence of an anion-binding site in NSMOA (Figure 8). In addition, we find that the observed rate constant for the flavin epoxidation reaction decreases with sodium chloride concentration. In this case, the observed rate constant appears to decrease linearly with salt concentration. However, this may represent the first part of a much weaker binding interaction in which the saturation component of the hyperbolic isotherm cannot be detected in the salt concentration range of 0−1 M.

Activation Parameters of the Transition States in the Reaction of NSMOA(FAD_{red}) with Styrene and Oxygen. Values of activation free energies listed in Table 2 were used together with estimated differences in energies of reaction intermediates

Scheme 2: Reaction Coordinate for the Epoxidation of Styrene by NSMOA

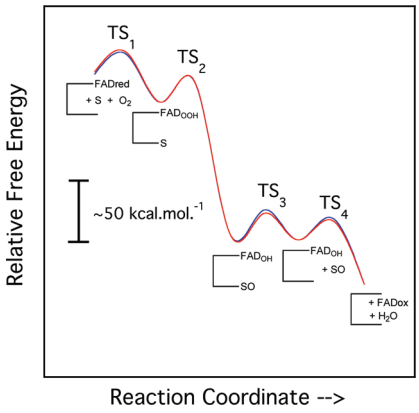

calculated from equilibrium constants for the binding of oxidized and reduced flavin and substrate to NSMOA (*16*) and estimated changes in chemical bond energies (*42*) associated with the transformations relating each intermediate state to construct the approximate reaction coordinate presented in Scheme 2. Because the dependence of activation free energy on pH is relatively small compared to the overall energetic change in the epoxidation reaction (Table 2), plots corresponding to the reaction proceeding at high and low pH appear to nearly superimpose. The largest change in free energy in this reaction is coupled styrene oxide dissociation in the transformation of the first intermediate to the second intermediate. This is followed by a significantly smaller change in free energy coupled to the elimination of water from the C(4a)-hydroxyflavin.

Kinetically Resolved pK_a Values in the Reaction Mechanism of NSMOA. The macroscopic pK_a values in this mechanism are quite similar and in the basic pH range. van't Hoff analysis (Table 3) indicates ionization enthalpies for deprotonation ranging from 8 to 28 kcal/mol, which are large and suggest the existence of multiple linked protic equilibria contributing to each of the observed macroscopic pK_a values (*43*). van't Hoff plots of pK_{a1} and pK_{a2} are not very linear and were determined over a narrow temperature range. More data recorded over a broader temperature range are required to evaluate the significance of this observation. The exact chemical species contributing to the kinetically resolved macroscopic pK_a values cannot be rigorously addressed at this time, but in considering the dependence of the observed rate constants on these pK_a values, we can conclude that the epoxidation reaction is acid-catalyzed whereas formation of flavin peroxide intermediate, elimination of water from the flavin hydroxide intermediate, and the dissociation of oxidized FAD from the enzyme at the end of the single-turnover reaction are all base-catalyzed (Figure 3).

It is likely that the macroscopic pK_a for C(4a)-flavinperoxide formation (pK_{a1} = 7.2) is linked to the protonation state of the isoalloxazine ring nitrogen [N(1)] or an ionizable active site base that interacts with this ring position (Scheme 1). Deprotonation of this position will increase electron density at the C(4a) position and increase the reactivity of the flavin with oxygen.

The macroscopic pK_a of the epoxidation reaction (pK_{a2} = 7.7) may be related to functional groups in the active site that tune the reactivity of the FAD C(4a)-peroxide. As shown in Scheme 1, the pK_a of C(4a)-flavin peroxide is estimated to be ~10 (*44*), but the active sites of flavin monooxygenases must be able to tune this value considerably to meet mechanistic demands. In the reactions

of aromatic ring hydroxylases, such as 4-hydroxybenzoate 3-monooxygenase (*24*, *45*), and phenol hydroxylase (*23*), the aromatic ring of the substrate is thought to make a nucleophilic attack on the protonated oxygen atom of the peroxide. Alternatively, bacterial luciferase (*46*), cyclohexanone (*21*), and alkane sulfonate (*47*) monooxygenases appear to effectively decrease the pK_a to yield a reactive anionic flavin peroxide intermediate that attacks substrate in a Bayer−Villiger-type mechanism.

In the case of cyclohexanone monooxygenase, deprotoation of the flavin hydroperoxide yields an anionic flavin peroxide that is coupled to a red shift in the absorbance maximum (*21*). The spectrum of the flavin peroxide form of NSMOA generated in the absence of styrene remains unchanged as a function of pH (Figure 4). Because we do not observe this spectral shift in the case of NSMOA, it is possible that the peroxide anion does not form at all in the active site environment provided by NSMOA, and the observed decrease in the epoxidation rate constant as a function of pH supports the FAD C(4a)-hydroperoxide being the reactive intermediate. The nature of this reaction intermediate may be better resolved through studies with nucleophilic and electrophilic styrene analogues and FAD analogues designed to react and generate C(4a)-peroxides spanning a range of electrophilicities (*45*).

The rate of elimination of water from the hydroxyflavin intermediate of the single-component phenol hydroxylase from *Trichosporon cutanium* is thought to be triggered by abstraction of a proton from the N(5) ring position by hydroxide ion in the active site (*25*). We hypothesize that the pK_{a3} of 8.3 and the pK_{a4} of 7.7 similarly represent pK_a values associated with the N(5) position of the C(4a)-FAD hydroxide intermediate of NSMOA in the presence and absence, respectively, of bound styrene oxide. Deprotonation of an active site residue in the proximity of position N(5) of the flavin in the presence of styrene oxide (pK_{a3} = 8.3) would generate negative charge in the vicinity of the oxide ring, decreasing the affinity of bound styrene oxide through electrostatic repulsion. We further propose that the product dissociation equilibrium constant may be linked to pK_{a3} such that the product dissociation is coupled to a decrease in this pK_a from 8.3 to a pK_{a4} of 7.6. Following the dissociation of the styrene oxide product, the rate constant for the elimination of water from the FAD C(4a)-hydroxide in the regeneration of oxidized FAD may then be controlled by pK_{a4} (Scheme 1).

ACKNOWLEDGMENT

We thank Drs. Jim Keeffe and Ihsan Erden for many insightful discussions and Dr. Pete Palmer for his expertise and assistance with the GC−MS instrument.

REFERENCES

1. Timmis, K. N. (2002) *Pseudomonas putida*: A cosmopolitan opportunist par excellence. *Environ. Microbiol. 4*, 779–781.
2. Hartmans, S., van der Werf, M. J., and de Bont, J. A. (1990) Bacterial degradation of styrene involving a novel flavin adenine dinucleotide-dependent styrene monooxygenase. *Appl. Environ. Microbiol. 56*, 1347–1351.
3. Nogales, J., Macchi, R., Franchi, F., Barzaghi, D., Fernandez, C., Garcia, J. L., Bertoni, G., and Diaz, E. (2007) Characterization of the last step of the aerobic phenylacetic acid degradation pathway. *Microbiology 153*, 357–365.
4. Di Gennaro, P., Ferrara, S., Ronco, I., Galli, E., Sello, G., Papacchini, M., and Bestetti, G. (2007) Styrene lower catabolic pathway in *Pseudomonas fluorescens* ST: Identification and characterization of genes for phenylacetic acid degradation. *Arch. Microbiol. 188*, 117–125.
5. van Hellemond, E. W., Janssen, D. B., and Fraaije, M. W. (2007) Discovery of a novel styrene monooxygenase originating from the metagenome. *Appl. Environ. Microbiol. 73*, 5832–5839.
6. Santos, P. M., Blatny, J. M., Di Bartolo, I., Valla, S., and Zennaro, E. (2000) Physiological analysis of the expression of the styrene degradation gene cluster in *Pseudomonas fluorescens* ST. *Appl. Environ. Microbiol. 66*, 1305–1310.
7. Panke, S., Wubbolts, M. G., Schmid, A., and Witholt, B. (2000) Production of enantiopure styrene oxide by recombinant *Escherichia coli* synthesizing a two-component styrene monooxygenase. *Biotechnol. Bioeng. 69*, 91–100.
8. Panke, S., Held, M., Wubbolts, M. G., Witholt, B., and Schmid, A. (2002) Pilot-scale production of (S)-styrene oxide from styrene by recombinant *Escherichia coli* synthesizing styrene monooxygenase. *Biotechnol. Bioeng. 80*, 33–41.
9. Otto, K., Hofstetter, K., Rothlisberger, M., Witholt, B., and Schmid, A. (2004) Biochemical characterization of StyAB from *Pseudomonas* sp. strain VLB120 as a two-component flavin-diffusible monooxygenase. *J. Bacteriol. 186*, 5292–5302.
10. Hollmann, F., Hofstetter, K., Habicher, T., Hauer, B., and Schmid, A. (2005) Direct electrochemical regeneration of monooxygenase subunits for biocatalytic asymmetric epoxidation. *J. Am. Chem. Soc. 127*, 6540–6541.
11. Hollmann, F., Lin, P. C., Witholt, B., and Schmid, A. (2003) Stereospecific biocatalytic epoxidation: The first example of direct regeneration of a FAD-dependent monooxygenase for catalysis. *J. Am. Chem. Soc. 125*, 8209–8217.
12. Feenstra, K. A., Hofstetter, K., Bosch, R., Schmid, A., Commandeur, J. N., and Vermeulen, N. P. (2006) Enantioselective substrate binding in a monooxygenase protein model by molecular dynamics and docking. *Biophys. J. 91*, 3206–3216.
13. Park, J. B., Buhler, B., Habicher, T., Hauer, B., Panke, S., Witholt, B., and Schmid, A. (2006) The efficiency of recombinant *Escherichia coli* as biocatalyst for stereospecific epoxidation. *Biotechnol. Bioeng. 95*, 501–512.
14. Kantz, A., Chin, F., Nallamothu, N., Nguyen, T., and Gassner, G. T. (2005) Mechanism of flavin transfer and oxygen activation by the two-component flavoenzyme styrene monooxygenase. *Arch. Biochem. Biophys. 442*, 102–116.
15. Tischler, D., Eulberg, D., Lakner, S., Kaschabek, S. R., van Berkel, W. J., and Schlomann, M. (2009) Identification of a novel self-sufficient styrene monooxygenase from *Rhodococcus opacus* 1CP. *J. Bacteriol. 191*, 4996–5009.
16. Ukaegbu, U. E., Kantz, A., Beaton, M., Gassner, G. T., and Rosenzweig, A. C. (2010) Structure and ligand binding properties of the epoxidase component of styrene monooxygenase. *Biochemistry 49*, 1678–1688.
17. Panke, S., Witholt, B., Schmid, A., and Wubbolts, M. G. (1998) Towards a biocatalyst for (S)-styrene oxide production: Characterization of the styrene degradation pathway of *Pseudomonas* sp. strain VLB120. *Appl. Environ. Microbiol. 64*, 2032–2043.
18. Buch, K., Stransky, H., and Hager, A. (1995) FAD is a further essential cofactor of the NAD(P)H and O_2-dependent zeaxanthin-epoxidase. *FEBS Lett. 376*, 45–48.
19. Laden, B. P., Tang, Y., and Porter, T. D. (2000) Cloning, heterologous expression, and enzymological characterization of human squalene monooxygenase. *Arch. Biochem. Biophys. 374*, 381–388.
20. Galan, B., Diaz, E., Prieto, M. A., and Garcia, J. L. (2000) Functional analysis of the small component of the 4-hydroxyphenylacetate 3-monooxygenase of *Escherichia coli* W: A prototype of a new flavin:NAD(P)H reductase subfamily. *J. Bacteriol. 182*, 627–636.
21. Sheng, D., Ballou, D. P., and Massey, V. (2001) Mechanistic studies of cyclohexanone monooxygenase: Chemical properties of intermediates involved in catalysis. *Biochemistry 40*, 11156–11167.
22. Vervoort, J., Muller, F., Lee, J., van den Berg, W. A. M., and Moonen, C. T. W. (1986) Identifications of the true carbon-13 nuclear magnetic resonance spectrum of the stable intermediate II in bacterial luciferase. *Biochemistry 25*, 8062–8067.
23. Maeda-Yorita, K., and Massey, V. (1993) On the reaction mechanism of phenol hydroxylase. New information obtained by correlation of fluorescence and absorbance stopped flow studies. *J. Biol. Chem. 268*, 4134–4144.
24. Entsch, B., Ballou, D. P., and Massey, V. (1976) Flavin-oxygen derivatives involved in hydroxylation by p-hydroxybenzoate hydroxylase. *J. Biol. Chem. 251*, 2550–2563.
25. Taylor, M. G., and Massey, V. (1990) Decay of the 4a-hydroxy-FAD intermediate of phenol hydroxylase. *J. Biol. Chem. 265*, 13687–13694.
26. Detmer, K., and Massey, V. (1984) Effect of monovalent anions on the mechanism of phenol hydroxylase. *J. Biol. Chem. 259*, 11265–11272.

27. Orf, H. W., and Dolphin, D. (1974) Oxaziridines as possible intermediates in flavin monooxygenases. *Proc. Natl. Acad. Sci. U.S.A. 71*, 2646–2650.
28. Houk, K. N., Liu, DeMello, N. C., and Condroski, K. R. (1997) Transition States of Epoxidations: Diradical Character, Spiro Geometries, Transition State Flexibility, and the Origins of Stereoselectivity. *J. Am. Chem. Soc. 119*, 10147–10152.
29. Davis, F. A., Harakal, M. E., and Awad, S. B. (1983) Chemistry of Oxaziridines. 4. Asymmetric Epoxidation of Unfunctionalized Alkenes Using Chiral 2-Sulfonyloxaziridines: Evidence for a Planar Transistion State Geometry. *J. Am. Chem. Soc. 105*, 3123–3126.
30. Steinfeld, J. I., Francisco, J. S., and Hase, W. L. (1989) Chemical Kinetics and Dynamics, Prentice Hall, Englewood Cliffs, NJ.
31. Winzor, D. J., and Jackson, C. M. (2006) Interpretation of the temperature dependence of equilibrium and rate constants. *J. Mol. Recognit. 19*, 389–407.
32. Massey, V. (1994) Activation of molecular oxygen by flavins and flavoproteins. *J. Biol. Chem. 269*, 22459–22462.
33. Suske, W. A., van Berkel, W. J., and Kohler, H. P. (1999) Catalytic mechanism of 2-hydroxybiphenyl 3-monooxygenase, a flavoprotein from *Pseudomonas azelaica* HBP1. *J. Biol. Chem. 274*, 33355–33365.
34. Tu, S. C. (1979) Isolation and properties of bacterial luciferase-oxygenated flavin intermediate complexed with long-chain alcohols. *Biochemistry 18*, 5940–5945.
35. Kurfurst, M., Ghisla, S., and Hastings, W. J. (1984) Characterization and postulated structure of the primary emitter in the bacterial luciferase reaction. *Proc. Natl. Acad. Sci. U.S.A. 81*, 2990–2994.
36. Chaiyen, P., Brissette, P., Ballou, D. P., and Massey, V. (1997) Unusual mechanism of oxygen atom transfer and product rearrangement in the catalytic reaction of 2-methyl-3-hydroxypyridine-5-carboxylic acid oxygenase. *Biochemistry 36*, 8060–8070.
37. Sucharitakul, J., Chaiyen, P., Entsch, B., and Ballou, D. P. (2006) Kinetic mechanisms of the oxygenase from a two-component enzyme, p-hydroxyphenylacetate 3-hydroxylase from *Acinetobacter baumannii*. *J. Biol. Chem. 281*, 17044–17053.
38. Jones, K. C., and Ballou, D. P. (1986) Reactions of the 4a-hydroperoxide of liver microsomal flavin-containing monooxygenase with nucleophilic and electrophilic substrates. *J. Biol. Chem. 261*, 2553–2559.
39. Ghisla, S., Entsch, B., Massey, V., and Husein, M. (1977) On the structure of flavin-oxygen intermediates involved in enzymatic reactions. *Eur. J. Biochem. 76*, 139–148.
40. Detmer, K., and Massey, V. (1985) Effect of substrate and pH on the oxidative half-reaction of phenol hydroxylase. *J. Biol. Chem. 260*, 5998–6005.
41. Schopfer, L. M., and Massey, V. (1980) Kinetic and mechanistic studies on the oxidation of the melilotate hydroxylase·2-OH-cinnamate complex by molecular oxygen. *J. Biol. Chem. 255*, 5355–5363.
42. Weast, R. C., Ed. (1986) Handbook of Chemistry and Physics, 67th ed., CRC Press, Inc., Boca Raton, FL.
43. Goldberg, R. N., Kishore, N., and Lennen, M. (2002) Thermodynamic quantities for the ionization reactions of buffers. *J. Phys. Chem. Ref. Data 31*, 231–370.
44. Schreuder, H. A., Hol, W. G., and Drenth, J. (1990) Analysis of the active site of the flavoprotein p-hydroxybenzoate hydroxylase and some ideas with respect to its reaction mechanism. *Biochemistry 29*, 3101–3108.
45. Ortiz-Maldonado, M., Ballou, D. P., and Massey, V. (1999) Use of free energy relationships to probe the individual steps of hydroxylation of p-hydroxybenzoate hydroxylase: Studies with a series of 8-substituted flavins. *Biochemistry 38*, 8124–8137.
46. Hastings, B. C. (1975) The oxygenated bacterial luciferase-flavin intermediate. *J. Biol. Chem. 250*, 7288–7293.
47. Zhan, X., Carpenter, R. A., and Ellis, H. R. (2008) Catalytic importance of the substrate binding order for the $FMNH_2$-dependent alkanesulfonate monooxygenase enzyme. *Biochemistry 47*, 2221–2230.